Boundary-Layer Meteorology
https://doi.org/10.1007/s10546-020-00533-w

RESEARCH ARTICLE

Non-stationary Boundary Layers

L. Mahrt[1] · **Elie Bou-Zeid**[2]

Received: 30 December 2019 / Accepted: 19 May 2020

Abstract
The literature includes a wide variety of definitions or perceptions of non-stationarity. Non-stationarity can be expressed in terms of turbulence statistics or variability of the forcing of the turbulence such as time changes of the wind vector, the horizontal pressure gradient, or the surface heat flux. Our survey emphasizes the development of non-equilibrium turbulence caused by non-stationary forcing. The degree of non-equilibrium of the turbulence is most reliably evaluated following the local flow rather than using the more available fixed-point measurements. We survey methods to eliminate non-stationary records or partially filter out the non-stationarity. We also summarize issues with parametrization of the non-stationarity. Non-stationarity over the sea can be complex due to time-dependent wave state and surface roughness. The impact of non-stationarity is generally less understood in the stable boundary layer compared to the unstable boundary layer.

Keywords Equilibrium turbulence · Non-stationarity · Spectral gap · Submeso · Turbulence adjustment

1 Introduction

The term *non-stationary* is defined in different ways and on different scales. Non-stationarity may refer to the turbulence statistics or to the non-turbulent flow that forces the turbulence. For some investigations, examination of non-stationarity is motivated by possible violation of similarity theory (e.g., Smeets et al. 1998). Our review focuses on the impact of the non-stationary wind field on the turbulence and whether the turbulence can maintain quasi-equilibrium with the changing flow.

Boundary-layer stationarity is often approximately valid in certain situations such as the polar night (Yagüe and Cano 1994; Grachev et al. 2007; Petenko et al. 2019), although sometimes wave-like motions are important. Stationarity is also common in open-ocean conditions where the diurnal forcing is small. Stationarity additionally requires relatively steady horizontal pressure gradients.

✉ L. Mahrt
mahrt@nwra.com

[1] NorthWest Research Associates, 2171 NW Kari Pl, Corvallis, OR 97330, USA

[2] Department of Civil and Environmental Engineering, Princeton University, Princeton, NJ 08544, USA

Published online: 15 June 2020

Frequently, the turbulence becomes non-stationary in response to time changes of the surface heat flux (thermal forcing). The diurnal trend with clear skies includes concentrated rapid changes of the thermal forcing during the late-afternoon transition to stable flow (Lothon et al. 2014; Angevine et al. 2020) and the morning transition to unstable flow (Hicks et al. 2018). To a lesser degree, the heat flux during the day is also non-stationary as it increases, reaches a maximum sometime after solar noon, and subsequently decreases with time, causing the turbulence intensity to decrease (Grimsdell and Angevine 2002; Nilsson et al. 2016). During both the evening and morning transitions, the relationships for equilibrium turbulence can break down (Hicks et al. 2018). The elimination of the morning surface inversion is typically more abrupt than predicted by the surface heat flux alone due to the downward entrainment of warmer air (Angevine et al. 2020).

Individual cloud elements commonly force important variations of the surface radiation balance for both unstable and stable conditions. The impact on the turbulence is sometimes difficult to establish from observations at a fixed site, particularly if the cloud elements are moving in a different direction from the surface wind direction. That is, the upwind history of the thermal forcing of the turbulence may be quite different from that inferred from fixed-point measurements. This complex cloud contribution to non-stationarity is outside the scope of our survey.

The non-stationarity is also driven by time-dependent horizontal pressure gradients (dynamic forcing), as in Momen and Bou-Zeid (2017b). Non-stationary modes are associated with propagating submeso motions, mesoscale disturbances, and synoptic fronts. Submeso motions include scales up to the smallest mesoscale motions typically on time scales of one hour, or horizontal scales of several kilometres, depending on the study. Non-stationary submeso motions often propagate and include smooth wave-like modes, sharp microfronts, and numerous more complex modes (e.g., Monti et al. 2002; Acevedo et al. 2014; Mahrt 2014; Sun et al. 2015a, b; Vercauteren et al. 2016; Cava et al. 2017; Mortarini et al. 2018. Micro-cold events can sometimes be well defined with sharp edges and arrive as microfronts (Zeeman et al. 2015; Kang et al. 2015; Lang et al. 2018).

With stable stratification and low wind speeds, the submeso motions may be primarily horizontal (Kristensen et al. 1981; Lilly 1983; Anfossi et al. 2005; Mortarini et al. 2016). Horizontal two-dimensional modes can result from vertical decorrelation (Lilly 1983) associated with the conversion of vertical kinetic energy to potential energy in the presence of strong stable stratification. These conditions often include meandering of the wind vector, sometimes in layers. Locally generated large eddies in the stable boundary layer (SBL) also lead to non-stationary intermittent turbulence and non-compliance with similarity theory (Ansorge and Mellado 2016; Ansorge 2019). Cases where a scale gap occurs between the turbulence and the submeso motions increase the possibility of quasi-equilibrium turbulence. Examples of such quasi-equilibrium turbulence can be found in Vercauteren et al. (2016, 2019).

The non-stationary pressure gradients often generate non-turbulent motions on time scales just larger than the largest turbulent scales preventing a gap in scales. Figure 1 provides one example of partitioning the stable boundary layer into different regimes that recognizes non-stationarity. We define these regimes in terms of length scales, which must be somewhat inferential because the observations in the atmospheric boundary layer are primarily time series at fixed sites. For the SBL, the length scale of the largest turbulent eddies is chosen to be 10 m in Fig. 1, only as an example. This value decreases with the magnitude of the stability and increases with the height above the ground. In this example, the maximum horizontal length scale of the submeso motions is chosen to be the scale traditionally specified for the smallest mesoscale motions, approximately 2 km (Orlanski 1975).

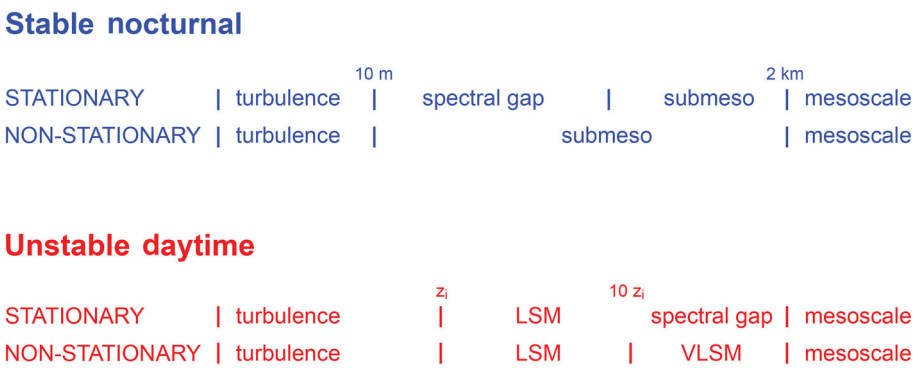

Fig. 1 Plausible, but simplified, scale dependence of the motions for stationary and non-stationary motions for stable and unstable boundary layers. The diagram is horizontally not to scale because the unstable regime encompasses a much larger range of scales. The terminology is imprecise and varies between studies. The horizontal length scales of 10 m and 2 km are only examples; z_i is the depth of the convective boundary layer

Figure 1 could be expanded by partitioning the SBL according to the strength of the stability (such as weakly stable and very stable classes) and could also be expanded according to height above the ground (surface layer, outer layer). These potential generalizations are excluded from our survey. Unlike the unstable boundary layer, the depth of the SBL is often not a useful scaling variable because some submeso motions are confined to near the surface while other submeso motions are much deeper than the perceived boundary-layer depth. In addition, the top of the SBL is often poorly defined.

For unstable conditions, the scale of the largest turbulent eddies can be one or more orders of magnitude larger than that for stable conditions. A spectral gap for the horizontal velocity components seems less common compared to the absence of a well-defined gap. Large boundary-layer eddies often eliminate the spectral gap between the turbulence and mesoscale motions, particularly for the horizontal velocity components (Kaimal et al. 1972; Kunkel and Marusic 2006).

Several different classification schemes have been developed for motions on scales larger than the largest turbulent eddies in the unstable boundary layer. We roughly follow the approach of Salesky and Anderson (2018) and Katul (2019), but do not review the origins of this thinking from the engineering fluid dynamics community (e.g., Smits et al. 2011). Salesky and Anderson (2018) and Katul (2019) have summarized much of this earlier material. The larger eddies are theoretically partitioned into large-scale motions (LSM) on scales comparable to the boundary-layer depth, z_i, and very large-scale motions (VLSM) that are order of 10 z_i where z_i is the depth of the unstable boundary layer. For near-neutral conditions, the dominant eddies are typically longitudinal vortices (Salesky et al. 2017). Based on the horizontal dimension in the downwind direction, these eddies are part of the VLSM regime (Salesky and Anderson 2018).

As the thermodynamic instability increases from neutral, the horizontal scale of the large eddies first increases and then subsequently decreases, and the motions become more isotropic in the horizontal direction (Shah and Bou-Zeid 2014; Salesky et al. 2017). The longitudinal eddies break down into disorganized convection as part of a dynamic–convective regime (Katul 2019), which might be considered as intermediate between the LSM and VLSM regimes. With convective conditions (large instability), the eddies become more like organized convection characterized by quasi-isotropy in the horizontal direction. These eddies are

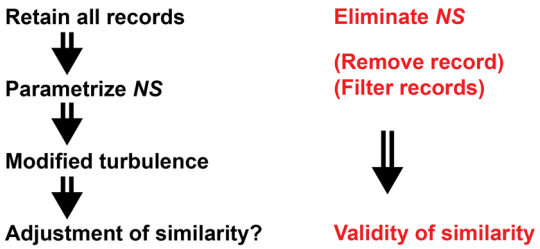

Fig. 2 The left-hand side (black) broadly identifies the approach where all measurements are retained while the the right-hand side (red) identifies the common approach where non-stationarity is at least partially removed. The path on the left-hand side has received only nominal quantitative attention. *NS* refers to non-stationarity. Parametrization of the non-stationary motions are briefly discussed in Sect. 8 while the corresponding modification of the turbulence is explored in Sects. 2 and 3. Filtering of records to reduce the non-stationarity and the complete removal of non-stationary records are both discussed in Sect. 5

in the LSM regime. Such convective boundary-layer scale eddies are generally considered part of the turbulence but sometimes parametrized separately (Beljaars 1995). We consider the LSM regime to be part of the turbulence in the most general sense but find that distinction between such a LSM regime and the "rest" of the turbulence can be useful. Non-stationary motions in the unstable boundary layer can also be forced by perturbation pressure gradients at or above the boundary-layer top associated with wave modes. Such waves may be coupled to the convective boundary-layer eddies (Kuettner et al. 1987).

Longitudinal vortices occur over a large range of horizontal scales. Hairpin vortices occur on a variety of scales and include smaller scales where the vortices are attached to the surface and generally included as part of the turbulence (Hutchins et al. 2012; Li and Bou-Zeid 2013). They may coalesce into larger vortices that could be classified as the LSM regime. Streamline-aligned roll vortices sometimes develop in association with Ekman instability (LeMone 1973, 1976; Brown 1980). These vortices are relatively low frequency when observed at a fixed point as the vortices slowly drift in the cross-wind direction. The along-wind length scale can significantly exceed $10z_i$, depending on the synoptic situation. Such vortices could be considered as the VLSM regime. Transverse vortices (Boppe et al. 1999) are characterized by a small length scale in the along-wind direction and a larger length scale in the cross-wind direction. These motions appear to be less common than the longitudinal motions.

Although the above classification schemes organize our thinking, they are not unique and are also incomplete compared to actual atmospheric flows. Furthermore, it is not possible to review the literature with a single definition of the non-stationarity. In simple terms, our review of disruption of turbulence equilibrium is broadly guided by the left-hand side of Fig. 2.

2 Equilibrium and Non-equilibrium Turbulence

We first offer a conceptual framework of equilibrium and non-equilibrium turbulence.

2.1 Lagrangian Versus Eulerian

Consider idealized stationary flow where the horizontal variation of the turbulence is negligible, which is a stronger assumption (more restrictive) than the assumption of surface

homogeneity. Then, Eulerian stationarity at a fixed point implies Lagrangian stationarity, and Lagrangian stationarity implies Eulerian stationarity.

In general, the turbulent eddies moving with the flow may experience much different non-stationarity than that inferred from observations at a fixed site. Consider a simple disturbance with enhanced turbulence that is propagating at the same speed as the local wind speed (Fig. 3a). Turbulence equilibrium is not determined by how long the enhanced turbulence requires to pass the fixed observational site but rather by how long the turbulence has been adjusting to the wind field of the propagating disturbance. From another point of view, quasi-equilibrium turbulence requires that the turbulence adjustment time scale is small compared to the lifetime of the disturbance and must be formally evaluated moving with the turbulence (*Lagrangian stationarity*). Even if this stationarity condition is satisfied, the Eulerian observations at a fixed site indicate non-stationarity where the observed turbulence increases with time, reaches a maxima, and then decreases with time as the disturbance passes the fixed observational point (Fig. 3a).

A common reverse example, where the flow is Lagrangian non-stationary with non-equilibrium turbulence but Eulerian stationary, occurs with flow over a surface roughness or temperature change (Garratt 1990, 1994). The turbulence is not in equilibrium but rather decays as it transitions to a smoother surface (Fig. 3b). However, as observed at a fixed site, the turbulence is independent of time, giving the false impression of equilibrium turbulence.

The assumption that a disturbance with enhanced turbulence propagates with the local mean flow can be a poor approximation for some situations. If a disturbance in the pressure field is propagating at a speed and direction different from the local wind vector (Rees et al. 2000; Mahrt et al. 2009; Lang et al. 2018), then the turbulence may no longer be Lagrangian stationary nor Eulerian stationary. A common example is a wave-like mode that propagates through the flow.

2.2 Equilibrium Requirements

Quantification of "quasi equilibrium" formally requires observations in a Lagrangian framework. The evolution of the eddies can be viewed to some degree in the Lagrangian framework through remote sensing of eddies (Higgins et al. 2012) and through fibre-optic measurements (Thomas et al. 2012; Zeeman et al. 2015; Pfister et al. 2019) for cases where the wind vector is aligned with the vertical plane of the observations. Unmanned aircraft also offer potential assessment of short-term evolution of the spatial variability near the surface (e.g., de Boer et al. 2018).

In the usual absence of such measurements, non-equilibrium turbulence is tentatively inferred from fixed-point measurements, as discussed below. With fixed-point measurements, the horizontal length scale of the dominant eddies, ℓ, can be estimated as $U\tau_p$ where τ_p is the time scale for the eddies to pass the fixed point and U is the local wind speed. This approximation requires that

$$\tau_p << \tau_{adj}, \tag{1}$$

where τ_{adj} is the eddy adjustment time scale. That is, Eq. (1) assumes that the dominant eddies do not evolve significantly during the time it takes them to pass the tower, as if they were "frozen." This can be viewed as a consequence of Taylor's hypothesis.

Turbulence quasi-equilibrium requires that the eddy adjustment time scale, τ_{adj}, is small compared to the time scale of the smallest significant non-turbulent motions characterized by time scale τ_{sm}. The adjustment time scale τ_{adj} might be related to the time scale of the

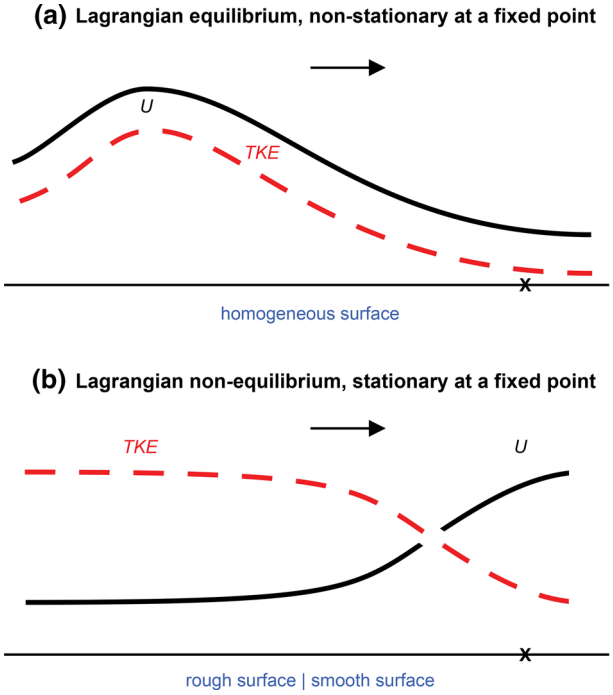

Fig. 3 **a** Idealized ensemble horizontal structure of turbulence (red dashed line, arbitrary units) is in equilibrium with the moving frozen structure of the mean flow (black solid line, arbitrary units), but is statistically perceived at a fixed point (X) as non-stationary flow with inferred non-equilibrium turbulence. **b** Flow over a heterogeneous surface is perceived as stationary at a fixed point (X) but in fact corresponds to non-equilibrium turbulence

large eddies, τ_t, which is written in terms of the simplest possible dimensional argument (Tennekes and Lumley 1972; Kaimal and Finnigan 1994) as

$$\tau_t \equiv C_e \ell / u_e, \tag{2}$$

where ℓ and u_e are the length scale and velocity scale of the dominant eddies, respectively, and C_e is a non-dimensional coefficient that could be nominally set to unity. As one example, u_e could be chosen as the surface friction velocity. The eddy size, ℓ, is sometimes assumed to be proportional to the boundary-layer depth.

Relating τ_{adj} to τ_t, and assuming quasi-equilibrium turbulence such that $\tau_{adj} << \tau_{sm}$, we obtain

$$\tau_t << \tau_{sm}, \tag{3}$$

where τ_{sm} describes the time scale of the smallest important non-turbulent flow.

The time scale τ_t, when estimated from the friction velocity and boundary-layer depth, represents the adjustment time of the largest eddies. However, the full spectrum of turbulent eddies might be adjusting with different time scales (Momen and Bou-Zeid 2017b). Therefore, the condition expressed in Eq. 3 might be insufficient for some purposes, depending on how the flow is evolving. For example, if the bulk mean shear suddenly changes through a change in the pressure forcing, the large structures are affected first and adjust with a time scale $\sim \tau_t$. However, because the smaller and smaller scales that feed on the energy of these larger scales

sequentially equilibrate, the equilibration of the full spectrum requires a time scale that is longer than τ_t.

If the forcing is completely removed, the full decay of turbulence requires the long time scale of l^2/ν (Tennekes and Lumley 1972). On the other hand, if static stability is abruptly introduced, it acts directly on smaller scales down to the Dougherty–Ozmidov scale (Dougherty 1961), and the spectrum might equilibrate faster than suggested by τ_t because the smaller scales have shorter eddy turnover time.

Analogous to the adjustment time scale, the relaxation time scale is often invoked in Rotta-type models of the pressure redistribution terms where $\tau_r \equiv e/\varepsilon$, where the turbulence kinetic energy (TKE, e) and dissipation rate (ε) vary with scale. See Katul et al. (2014) and references therein. This relaxation scale is also intended to express how rapidly eddies equilibrate by returning to isotropy. In spectral models of the redistribution, formulation of this relaxation time makes its dependence on scale or wavenumber k more explicit, (e.g., $\tau_r(k) \sim k^{-2/3}\varepsilon^{-1/3}$).

In practice, the input quantities for the above time scales are difficult to estimate from geophysical time series. Normally, non-equilibrium turbulence is inferred from surrogate calculations as outlined below.

3 Generation of Non-equilibrium Turbulence

Departure of the turbulence from equilibrium with non-stationary motions can be most fundamentally examined in terms of forcing by time-dependent horizontal pressure gradients or a time-dependent surface heat flux in a numerical setting where the physics can be at least partially isolated. Momen and Bou-Zeid (2017b) explicitly identified the role of the time scale of a specified non-stationary horizontal pressure gradient. When the time scale of the forcing by the horizontal pressure gradient is large compared to the characteristic time scale of the turbulence (a scale gap), the turbulence maintains quasi-equilibrium with the forcing. In contrast, the turbulence does not maintain equilibrium when the forcing time scale is the same order of magnitude as the time scale of the main turbulence eddies.

The very stable boundary layer can be considerably more complex where forcing may simultaneously occur on a variety of scales, including scales just larger than the turbulence. However, new stochastic analyses are providing valuable insight into the generation of turbulence by non-stationary motions, including possible switching back and forth between different states (McNider et al. 1995; Sun et al. 2012; Monahan et al. 2015; Kang et al. 2015; Vercauteren et al. 2016; Sun et al. 2016; Abraham and Monahan 2020). Through extended multiresolution analysis, Nilsson et al. (2013) were able to identify the generation of momentum flux due to specific scales of the non-turbulent submeso motions. The influence of non-stationary motions on the turbulence can also be viewed as externally forced turbulent intermittency (Monti et al. 2002; Yagüe et al. 2006; Acevedo et al. 2014; Sun et al. 2015a, b; Burman et al. 2018; Cava et al. 2019; Vercauteren et al. 2019) although the term "intermittency" varies substantially between studies.

The non-stationary motions can be partitioned into a deceleration phase and an acceleration phase where the impact on the turbulence is different. With flow deceleration, fluxes can be greater than equilibrium predictions due to frequent increasing directional shear with decreasing airflow, inflection point instability associated with flow distortion, and turbulence that is decaying but still influenced by previous higher wind speeds (Mahrt et al. 2013). That is, the turbulence intensity decreases during the deceleration phase, but remains larger than

the equilibrium value due to the lag of the of the decaying turbulence. With accelerating flow, the intensity of the lagging turbulence is less than the equilibrium value. On average, non-stationarity in the stable boundary layer can lead to a net increase in the turbulent transport (Mahrt 2008), although the generality of this result is not known. Salesky and Anderson (2018), and citations therein, find that LSM and VLSM can significantly modulate the amplitude of small-scale turbulent fluctuations.

Most observational studies do not consider the feedback of the turbulent fluxes upon the non-stationary motions. Increased turbulence and downward momentum flux can lead to flow acceleration such that cause-and-effect relations between the flow and turbulence become obscure or unexpected (Shah and Bou-Zeid 2014). Alternatively, the generation of significant mixing might eliminate or damp the non-stationary motions responsible for the turbulence generation and become the main cause of the turbulence demise.

4 Measures of Non-stationarity and Non-equilibrium Behaviour

How far can the flow depart from stationarity before the assumption of equilibrium turbulence becomes invalid? Yaglom (1973) formally defines and comprehensively discusses various degrees of stationarity: see also Tennekes and Lumley (1972), Panofsky and Dutton (1984), and Sorbjan (1989). For example, complete turbulence stationarity theoretically requires that the lagged autocorrelation coefficient depends only on the lag (for any lag) and not on the position in the time series. In other words, turbulent statistics for one part of the record should be the same as for any other part of the record. However, the estimate of these turbulent statistics requires a sufficiently long sub-record length so that the random errors are small for each sub-record, which in turn requires that the total record length is very long. Very long stationary records are difficult to find in the atmospheric boundary layer. In addition, evaluating the random error formally requires stationarity, leading to a circular problem.

The lack of an inertial subrange can be an indicator of important non-stationarity (Sorbjan and Grachev 2010; Grachev et al. 2013; Li et al. 2015). Li and Fu (2011) identified the impact of non-stationarity in terms of clustering and intermittency behaviour. Non-stationarity can also be inferred from sensitivity of the integral scale to the record length and failure to converge without filtering or conditioning of the data (Panofsky and Dutton 1984; Dias et al. 2018). Because of common non-stationarity, Panofsky and Dutton (1984) recommend avoiding integral scales for the analysis of atmospheric observations. Simiu et al. (2019) estimated the integral scale based on fitted spectra, though the behaviour of the integral scale may differ between different variables (Dias et al. 2004).

Non-stationarity is more commonly inferred from the lack of a spectral gap (Fig. 1), usually in terms of the horizontal velocity spectra. Spectral gaps above the boundary layer (in the free troposphere) are generally not evident (Nastrom and Gage 1985; Gage and Nastrom 1986), noting that spectral gaps are expected in stationary boundary layers. In stable boundary layers, Vercauteren et al. (2016) found a subclass of submeso motions that were separated in scale from the turbulent motions, allowing turbulence quasi-equilibrium. A subclass with an incomplete or non-existent spectral gap between the turbulent and non-turbulent motions suggests that the turbulence cannot maintain equilibrium with the submeso motions (Vercauteren et al. 2016). For very stable conditions over land, the lack of a spectral gap may be related to the obscurity of the transition between turbulent and non-turbulent scales, possibly due to scale overlap of the submeso motions and the turbulence. This regime is intrinsically non-stationary.

A spectral gap may be "shallow" in the unstable boundary layer corresponding to significant kinetic energy within the gap (Larsén et al. 2016). Panofsky and Dutton (1984), Schulz and Sanderson (2004), Lenschow and Sun (2007), Simiu et al. (2019), and citations therein, provide examples of poor or nonexistent scale gaps. Even though the spectral gap for the horizontal velocity components may be limited or missing, the cospectra may still be useful for identifying the turbulent scales. If the cospectra are poorly defined, the estimated turbulent fluxes become sensitive to the choice of averaging time (Schulz and Sanderson 2004).

One can consider dissipation/production of turbulence intensity and estimate how much these vary in time, and in equilibrium turbulence, these quantities, or at least their ratio, should be steady. Dissipation can be practically estimated from observations of structure functions. A basic test for equilibrium examines the potential production–dissipation balance of TKE, where dissipation is evaluated indirectly from observations (Freire et al. 2019) or non-equilibrium is evaluated directly from direct numerical simulations. Momen and Bou-Zeid (2017b) used the criterion that the ratio of the shear production to the dissipation for neutral conditions should remain ≈ 1 for turbulence to be in equilibrium with a varying mean flow. Cancelli et al. (2012) applied this test to scalars for unstable conditions and showed that strong vertical transport of scalar covariance disrupts the production–dissipation balance. This disruption violates Monin–Obukhov and temperature–humidity similarity theory. They also proposed dimensional indicators to gauge the effect of transport on the imbalance.

5 Removal of Non-stationarity

A number of less rigorous methods have been developed to quantify non-stationarity toward the goal of removing non-stationary records or attempting to "filter" out the non-stationary scales. While the removal of non-stationary records improves the performance of similarity theory, numerical models are often applied to all conditions, including non-stationary periods. As a result, similarity relationships calibrated to stationary conditions might lead to a flux bias when applied to all situations.

Methods to remove non-stationary records all make assumptions and generally require specification of threshold values. Večenaj and De Wekker (2015) and Babić et al. (2016) provide extensive surveys and examine a number of methods that allow objective removal of non-stationary records. Because the methods can disagree substantially, Večenaj and De Wekker (2015) simultaneously applied several methods to better ensure removal of the significant non-stationarity. Coulter and Doran (2002) removed records with large non-stationarity based on a measure of the intermittency and a threshold value. Violation of similarity theory can be dominated by large deviations of a limited number of individual points from similarity relationships (outliers), and such outliers contribute to the overall non-stationarity of the time series. Removal of outliers improves the performance of similarity but may exclude real behaviour.

Removal of the non-stationary scales from records without removing entire records is more complex. Filtering non-stationarity from the non-turbulent flow provides more meaningful fluxes by reducing the inadvertent non-turbulent contribution to the turbulent fluxes but does not remove the non-equilibrium character of the turbulence. Examples of filtering can be found in Večenaj and De Wekker (2015); detrending techniques are a form of filtering for removing non-stationarity (Rannik and Vesala 1999). Metzger and Holmes (2008) removed non-stationarity based on various characteristic time scales estimated from the time series. Based on a multi-resolution decomposition, Howell and Sun (1999) examined the flux

intermittency for each scale posed in terms of the standard error and filtered out the larger scales based on the standard error. Local wavelet transforms are particularly effective for examination of non-stationary turbulence (Collineau and Brunet 1993; Cornish et al. 2006; Metzger and Holmes 2008; Martins et al. 2017).

6 Non-stationary Mean Flows with Quasi-Equilibrium Turbulence

Although we focus primarily on deviation of the turbulence from an equilibrium state, we briefly examine non-stationarity on larger time scales where the turbulence may maintain quasi-equilibrium with the evolving flow. The non-stationarity of the mean flow on time scales much larger than the turbulent time scale and larger than the spectral gap, when it occurs, generally permits quasi-equilibrium turbulence and compliance with classical theories. Non-normalized turbulence statistics may still be unsteady. In many cases, these transient dynamics of the mean are the dominant characteristic of the flow and dictate the time dependence of the turbulence dynamics and surface fluxes.

During the evening transition, the decrease in turbulence intensity at any level can reduce the coupling with the surface, setting up an inertial oscillation whereby the flow above the surface accelerates significantly, producing a low-level jet. These dynamics were first modelled by Blackadar (1957) as an undamped oscillator where the eddy viscosity (and thus the stress-divergence term) is assumed to suddenly vanish at the idealized transition time. Improvement on this model was later obtained in terms of a sudden (Shapiro and Fedorovich 2010; Van de Wiel et al. 2010; Momen and Bou-Zeid 2016), or gradual (Momen and Bou-Zeid 2017a) reduction of the diffusivity. The transient response of the mean flow can then be predicted for any change in the balance between the pressure gradient, Coriolis, and friction forces (such as change of synoptic pressure gradient, decrease in the turbulent stress associated with increased stability, and so on).

The quasi-stationarity assumption is valid only if the forces change over sufficiently long time scales to maintain a spectral gap. Then classic turbulence closures can be used to develop Reynolds-averaged models of the time evolution of the mean wind vector. The mean flow also evolves sufficiently slowly to allow equilibrium turbulence in some katabatic flows (Shapiro and Fedorovich 2010), land-sea breezes (Gilliam et al. 2004), and possibly the response of the boundary layer to the passage of a synoptic frontal zone.

7 Over the Sea

The lack of a significant diurnal trend over the open ocean reduces one of the main causes of non-stationary airflow. However, non-stationarity of the wind field over the sea can lead to greater complexity compared to that over land surfaces because the wave state and surface roughness are jointly adjusting to the non-stationary wind field. Over land, the surface roughness at a fixed point is more or less constant, at least for a given wind direction. Non-stationarity of the airflow over the sea influences the surface stress both *directly* (as would occur with fixed surface roughness) and *indirectly* through modification of the surface wave field and surface roughness.

Different frequencies of the wave field respond differently to changes in the wind vector (Rieder and Smith 1998). The capillary waves and small gravity waves respond more quickly and more likely achieve quasi-equilibrium with the changing wind field, with the main wind-

driven waves and the swell requiring more time to adjust. Mahrt et al. (2016) found that for a given averaged wind speed, non-stationarity enhanced the sea-surface stress. Under low-wind conditions, Grachev et al. (2003) found that the non-stationarity of the airflow can generate large cross-wind stress angles. Chen et al. (2018), and citations therein, also show that non-stationarity of the wind field can cause large deviations of the direction of the sea-surface stress vector from the wind direction. They recommend routinely assessing the importance of the non-stationarity of the airflow.

8 Parametrization of the Non-stationary Motions

Unfortunately, the parametrization of the overall influence of the small-scale motions on the turbulence first requires predicting the non-stationary motions themselves. The causes of such motions are often unknown, and they may propagate from outside of the observational domain. Small-scale non-stationary motions are frequently not resolved by the spatial resolution of numerical models, are not included because of incomplete physics in the models, or are eliminated by implicit or explicit horizontal diffusion (Belušić and Güttler 2010; Güttler and Belušić 2012).

As a general indicator of non-stationarity evaluated from measurements in the SBL, Acevedo et al. (2014) defined the ratio $R_{sm} \equiv e_{sm}/\sigma_w^2$, where e_{sm} is the submeso kinetic energy and σ_w is the standard deviation of the vertical component of the turbulence. They find this ratio to increase with increasing stability. In some studies, the submeso kinetic energy e_{sm} increases only slowly with increasing wind speed, U, without any obvious dependence on stability (Anfossi et al. 2005). Vickers and Mahrt (2007) and Acevedo et al. (2014) found that, on average, e_{sm} is largest in complex terrain, smaller over flatter surfaces, and smallest over the sea. Because e_{sm} increases with the largest scale included in the calculation of e_{sm}, and because both U^2 and σ_w^2 can be relatively independent of this scale, the ratio R_{sm} increases with the largest scale included in the calculation of e_{sm}.

At the time of writing, progress is being made on the formulation of the non-stationary motions for the unstable boundary layer and their impact on the turbulent fluxes (personal communication, Scott Salesky 2020). This problem is better posed in the unstable boundary layer compared to the SBL because different types of non-stationary motions in the SBL are commonly superimposed and may originate non-locally.

9 Future Directions

Determination of the degree of equilibrium of the turbulence and the validity of similarity theory for the surface fluxes is an important motivation for assessing non-stationarity in boundary layers. Common causes of non-stationary turbulence are time-dependent thermal forcing and time-dependent dynamical forcing by motions on scales just larger than the largest turbulent eddies. Small-scale motions that dynamically force non-equilibrium turbulence are often unpredictable themselves.

The departure from equilibrium turbulence is not well understood, partly because existing observational systems do not allow following the modification of the turbulence by moving with the local flow. Measurements at fixed points reveal only "snapshots" of eddies or turbulent patches as they pass a fixed point, without adequate information on the generation of such turbulence upwind from the fixed point or the decay of such turbulence downwind from

the fixed point. Networks of observations over homogenous surfaces provide the opportunity to examine turbulence adjustment in a Lagrangian framework although such investigations remain for future work. Fibre-optic sensing and remote sensing by lidar can yield detailed insight into the evolution of the turbulence moving with the flow (Sect. 2.2).

Non-stationary submeso motions in the SBL are currently not well resolved or else poorly predicted by numerical models. These scales include a variety of different types of motion that include those that propagate over long distances. Progress may be afforded by detailed comparison of fields from model simulations with spatially-resolved observational networks that include a sufficiently large range of space scales. This allows the evaluation of the Lagrangian and Eulerian unsteadiness and associated disruption of turbulence equilibrium.

To organize future studies of the effect of non-stationarity, Fig. 1 provides a plausible non-unique classification of non-stationarity regimes. Is this preliminary classification scheme, or any classification scheme, useful for examining the degree of turbulence equilibrium and for estimating any systematic deviation of the fluxes from equilibrium values? Can Fig. 1 be improved and expanded to include transitional periods?

A general path of future investigations might follow the left-hand side of Fig. 2. The parametrization of the non-stationarity is expected to be only very approximate for the stable case but more tenable for the unstable case. Prediction of non-stationary motions is required to formulate modification of the turbulence and turbulent fluxes. The goal is to at least modestly improve upon the use of existing similarity theory. A more immediate short-term goal might be to pragmatically improve the prediction of similarity theory with simple adjustments of the coefficients to correct for "climatic bias", such as systematic underestimation of the surface stress. A longer term goal is to move toward understanding the full range of non-universal motions from the turbulence production range up to the mesoscale, and how they interact under non-equilibrium conditions.

Acknowledgements The comments of Scott Salesky and two reviewers are greatly appreciated. Larry Mahrt received support from Grants AGS-1614345 and 1945587 from the National Science Foundation.

References

Abraham C, Monahan A (2020) Climatological features of the weakly and very stably stratified nocturnal boundary layers Part III: the structure of meteorological state variables in persistent regime nights and across regime transitions. J Atmos Sci. https://doi.org/10.1175/JAS-D-18-0274.1

Acevedo O, Costa F, Oliveira P, Puhales F, Degrazia G, Roberti D (2014) The influence of submeso processes on stable boundary layer similarity relationships. J Atmos Sci 71:207–225

Anfossi D, Oetti D, Degrazia G, Boulart A (2005) An analysis of sonic anemometer observations in low wind speed conditions. Boundary-Layer Meteorol 114:179–203

Angevine W, Edwards JM, Lothon M, LeMone MA, Osborne SR (2020) Transition periods in the diurnally-varying atmospheric boundary layer over land. Boundary-Layer Meteorol. https://doi.org/10.1007/s10546-020-00515-y10.1175/2010MWR3142.1

Ansorge C (2019) Scale-dependence of atmosphere-surface coupling though similarity theory. Boundary-Layer Meteorol 170:1–27

Ansorge C, Mellado J (2016) Analyses of external and global intermittency in the logarithmic layer of Ekman flow. J Fluid Mech 805:611–635

Babić N, Večenaj Ž, De Wekker SFJ (2016) Flux-variance similarity in complex terrain and its sensitivity to different methods of treating non-stationarity. Boundary-Layer Meteorol 159:123–145

Beljaars A (1995) The parameterization of surface fluxes in large-scale models under free convection. Q J R Meteorol Soc 121:255–270

Belušić D, Güttler I (2010) Can mesoscale models reproduce meandering motions? Q J R Meteorol Soc 136:553–565

Blackadar A (1957) Boundary layer wind maxima and their significance for the growth of nocturnal inversions. Bull Am Meteorol Soc 38:283–290
Boppe RS, Neu WL, Shuai H (1999) Large-scale motions in the marine atmospheric surface layer. Boundary-Layer Meteorol 99:165–183
Brown R (1980) Longitudinal instabilities and secondary flows in the planetary boundary layer: a review. Rev Geophys 88(18):683–697
Burman PKD, Prabha TV, Morrison R, Karipot A (2018) A case study of turbulence in the nocturnal boundary layer during the Indian Summer Monsoon. Boundary-Layer Meteorol 169:115–138
Cancelli DM, Dias NL, Chamecki M (2012) Dimensionless criteria for the production-dissipation equilibrium of scalar fluctuations and their implications for scalar similarity. Water Resources Res 48:W10522. https://doi.org/10.1029/2012WR012127
Cava D, Mortarini L, Giostra U, Richiardone R, Anfossi D (2017) A wavelet analysis of low wind speed submeso motions in a nocturnal boundary layer. Q J R Meteorol Soc 143:661–669
Cava D, Mortarini L, Anfossi D, Giostra U (2019) Interaction of submeso motions in the Antarctic stable boundary layer. Boundary-Layer Meteorol 171:151–173
Chen S, Qiao F, Jiang Huang C, Zhao B (2018) Deviation of wind stress from wind direction under low wind conditions. J Geophys Res 123(12):9357–9368. https://doi.org/10.1029/2018JC014137
Collineau S, Brunet Y (1993) Detection of turbulent coherent motions in a forest canopy part I: Wavelet analysis. Boundary-Layer Meteorol 65:357–379
Cornish C, Bretherton C, Percival D (2006) Maximal overlap wavelet statistical analysis with applications to atmospheric turbulence. Boundary-Layer Meteorol 119:339–374
Coulter R, Doran J (2002) Spatial and temporal occurrences of intermittent turbulence during CASES-99. Boundary-Layer Meteorol 105:329–349
de Boer G, Ivey M, Schmid B, DeBaas DL, Driedonks AGM, Dexheimer D, Mei F, Hubbe J, Bendure A, Hardesty J, Shupe MD, McComiskey A, Telg H, Schmitt C, Matrosov S, Brooks I, Creamean J, Solomon A, C Williams DT, Maahn M, Argrow B, Palo S, Long C, Gao R, Mather J (2018) A bird's-eye view: Development of an operational ARM unmanned aerial capability for atmospheric research in Arctic Alaska. Bull Am Meteorol Soc 99:1197–2012
Dias N, Chamecki M, Kan A, Okawa C (2004) A study of spectra, structure and correlation functions and their implications for stationarity of surface-layer turbulence. Boundary-Layer Meteorol 110:165–189
Dias NL, Crivellaro BL, Chamecki M (2018) The Hurst phenomenon in error estimates related to atmospheric turbulence. Boundary-Layer Meteorol 168:387–416
Dougherty J (1961) The anisotropy of turbulence at the meteor level. J Atmos Terr Phys 21:210–213
Freire LS, Chamecki M, Bou-Zeid E, Dias NL (2019) Critical flux Richardson number for Kolmogorov turbulence enabled by TKE transport. Q J R Meteorol Soc 145:155–1558
Gage K, Nastrom G (1986) Theoretical interpretation of atmospheric wavenumber spectra of wind and temperature observed by commercial aircraft during gasp. J Atmos Sci 43:729–740
Garratt JR (1990) The internal boundary layer—a review. Boundary-Layer Meteorol 50:171–203
Garratt JR (1994) The atmospheric boundary layer. Cambridge University Press, Cambridge
Gilliam R, Raman S, Niyogi D (2004) Observational and numerical study on the influence of large-scale flow direction and coastline shape on sea-breeze evolution. Boundary-Layer Meteorol 2:275–300
Grachev A, Andreas E, Fairall C, Guest P, Persson P (2007) SHEBA flux profile relationship in the stable boundary layer. Boundary-Layer Meteorol 124:315–333
Grachev AA, Fairall CW, Hare JE, Edson JB, Miller SD (2003) Wind stress vector over ocean waves. J Phys Oceanogr 33:2408–2429
Grachev AA, Andreas E, Fairall C, Guest P, Persson P (2013) The critical Richardson number and limits of applicability of local similarity theory in the stable boundary layer. Boundary-Layer Meteorol 147:51–82
Grimsdell A, Angevine W (2002) Observations of the afternoon transition of the convective boundary layer. J Appl Meteorol 41:3–11
Güttler I, Belušić D (2012) The nature of small-scale non-turbulent variability in a mesoscale model. Atmos Sci Let 13(3):169–173. https://doi.org/10.1002/asl.382
Hicks BB, Pendergrass WR, Baker BD, Saylor RD, Dell DL, Eash NS, McQueen JT (2018) On the relevance of $\ln(z_0/z_{0T}) = \kappa\beta^{-1}$. Boundary-Layer Meteorol 167:285–301
Higgins CW, Froidevaux M, Simeonov V, Vercauteren N, Barry C, Parlange MB (2012) The effect of scale on the applicability of Taylor's frozen turbulence hypothesis in the atmospheric boundary layer. Boundary-Layer Meteorol 143:379–391
Howell J, Sun J (1999) Surface layer fluxes in stable conditions. Boundary-Layer Meteorol 90:495–520
Hutchins N, Chauhan K, Marusic I, Monty J, Klewicki J (2012) Towards reconciling the large-scale structure of turbulent boundary layers in the atmosphere an laboratory. Boundary-Layer Meteorol 145:273–306

Kaimal J, Finnigan J (1994) Atmospheric boundary layer flows: their structure and measurement. Oxford Press, Oxford
Kaimal J, Wyngaard JC, Izumi I, Coté Y (1972) Spectral characteristics of surface-layer turbulence. Q J R Meteorol Soc 98:563–589
Kang Y, Belušić D, Smith-Miles K (2015) Classes of structures in the stable atmospheric boundary layer. Q J R Meteorol Soc 141:2057–2069
Katul GG (2019) The anatomy of large-scale motion in atmospheric boundary layers. J Fluid Mech 858:1–4. https://doi.org/10.1017/jfm.2018.731
Katul GG, Porporato A, Shah S, Bou-Zeid E (2014) Two phenomenological constants explain similarity laws in stably stratified turbulence. Phys Rev E 89(2):023007. https://doi.org/10.1103/PhysRevE.89.023007
Kristensen L, Jensen N, Peterson EL (1981) Lateral dispersion of pollutants in a very stable atmosphere: the effect of the meandering. Atmos Environ 15:837–844
Kuettner J, Hildebrand P, Clark T (1987) Convection waves: observations of gravity wave systems over convectively active boundary layers. Q J R Meteorol Soc 113:445–467
Kunkel GJ, Marusic I (2006) Study of the near-wall-turbulent region of the high-reynolds-number boundary layer using an atmospheric flow. J Fluid Mech 548:375–402
Lang F, Belušić D, Siems S (2018) Observations of wind direction variability in the nocturnal boundary layer. Boundary-Layer Meteorol 166:51–68
Larsén XG, Larsen SE, Petersen EL (2016) Full-scale spectrum of boundary-layer winds. Boundary-Layer Meteorol 159:341–371
LeMone M (1973) The structure and dynamics of horizontal roll vortices in the planetary boundary layer. J Atmos Sci 30:1077–1091
LeMone M (1976) Modulation of turbulent energy by longitudinal rolls in an unstable planetary boundary layer. J Atmos Sci 33:1308–1320
Lenschow DH, Sun J (2007) The spectral composition of fluxes and variances over land and sea out to the mesoscale. Boundary-Layer Meteorol 125:63–84
Li D, Bou-Zeid E (2013) Coherent structures and the dissimilarity of turbulent transport of momentum and scalars in the unstable atmospheric boundary layer. Boundary-Layer Meteorol 149:219–230
Li Q, Fu Z (2011) The effects of non-stationarity on the clustering properties of the boundary-layer vertical wind velocity. Boundary-Layer Meteorol 140:243–262
Li D, Katul GG, Bou-Zeid E (2015) Turbulent energy spectra and cospectra of momentum and heat fluxes in the stable atmospheric surface layer. Boundary-Layer Meteorol 157:1–21
Lilly D (1983) Stratified turbulence and the mesoscale variability of the atmosphere. J Atmos Sci 40:749–761
Lothon M, Lohou F, Pino D, Couvreux F, Pardyjak ER, Reuder J, Vilà-Guerau de Arellano J, Durand P, Hartogensis O, Legain D, Augustin P, Gioli B, Lenschow DH, Faloona I, Yagüe C, Alexander DC, Angevine WM, Bargain E, Barrié J, Bazile E, Bezombes Y, Blay-Carreras E, van de Boer A, Boichard JL, Bourdon A, Butet A, Campistron B, de Coster O, Cuxart J, Dabas A, Darbieu C, Deboudt K, Delbarre H, Derrien S, Flament P, Fourmentin M, Garai A, Gibert F, Graf A, Groebner J, Guichard F, Jiménez MA, Jonassen M, van den Kroonenberg A, Magliulo V, Martin S, Martinez D, Mastrorillo L, Moene AF, Molinos F, Moulin E, Pietersen HP, Piguet B, Pique E, Román-Cascón C, Rufin-Soler C, Saïd F, Sastre-Marugán M, Seity Y, Steeneveld GJ, Toscano P, Traullé O, Tzanos D, Wacker S, Wildmann N, Zaldei A (2014) The BLLAST field experiment: boundary-layer late afternoon and sunset turbulence. Atmospheric Chemistry and Physics 14:10,931–10,960
Mahrt L (2008) The influence of transient flow distortion on turbulence in stable weak-wind conditions. Boundary-Layer Meteorol 127:1–16
Mahrt L (2014) Stably stratified atmospheric boundary layers. Annu Rev Fluid Mech 46:23–45
Mahrt L, Thomas CK, Prueger J (2009) Space-time structure of mesoscale modes in the stable boundary layer. Q J R Meteorol Soc 135:67–75
Mahrt L, Thomas CK, Richardson S, Seaman N, Stauffer D, Zeeman M (2013) Non-stationary generation of weak turbulence for very stable and weak-wind conditions. Boundary-Layer Meteorol 177:179–199
Mahrt L, Andreas EL, Edson JB, Vickers D, Sun J, Patton EG (2016) Coastal zone surface stress with stable stratification. J Phys Oceanogr 46:95–105
Martins L, Miller S, Acevedo O (2017) Using empirical mode decomposition to filter out non-turbulent contributions to air-sea fluxes. Boundary-Layer Meteorol 163:123–141
McNider R, England D, Friedman M, Shi X (1995) Predictability of the stable atmospheric boundary layer. J Atmos Sci 52:1602–1614
Metzger M, Holmes H (2008) Time scales in the unstable atmospheric surface layer. Boundary-Layer Meteorol 126:29–50
Momen M, Bou-Zeid E (2016) Large eddy simulations and damped-oscillator models of the unsteady Ekman boundary layer. J Atmos Sci 73:25–40

Momen M, Bou-Zeid E (2017a) Analytical reduced models for the non-stationary diabatic atmospheric boundary layer. Boundary-Layer Meteorol 164:383–399
Momen M, Bou-Zeid E (2017b) Mean and turbulence dynamics in unsteady Ekman boundary layers. J Fluid Mech 816:209–242
Monahan A, Rees T, He Y, McFarlane N (2015) Multiple regimes of wind, stratification, and turbulence in the stable boundary layer. J Atmos Sci 72:3178–3198
Monti PF, Chan W, Princevac M, Kowalewski T, Pardyjak E (2002) Observations of flow and turbulence in the nocturnal boundary layer over a slope. J Atmos Sci 59:2513–2534
Mortarini L, Stefanello M, Degrazia G, Roberti D, Castelli ST, Anfossi D (2016) Characterization of wind meandering in low-wind-speed conditions. Boundary-Layer Meteorol 161:165–182
Mortarini L, Cava D, Giostra U, Acevedo O, Nogueira Martins LG, Soares de Oliveira PE, Anfossi D (2018) Observations of submeso motions and intermittent turbulent mixing across a low level jet with a 132-m tower. Q J R Meteorol Soc 144:172–183
Nastrom G, Gage K (1985) A climatology of atmospheric wavenumber spectra of wind and temperature observed by commercial aircraft. J Atmos Sci 42:950–960
Nilsson E, Sahlée E, Rutgersson A (2013) Turbulent flux characterization using extended multiresolution analysis. Q J R Meteorol Soc 140:1715–1728
Nilsson E, Lohou F, Lothon M, Pardyjak E, Mahrt L, Darbieu C (2016) Turbulence kinetic energy budget during the afternoon transition—Part 1: observed surface tke budget and boundary layer description for 10 intensive observation period days. Atmospheric Chemistry and Physics 16:8849–8872
Orlanski I (1975) A rational subdivision of scales for atmospheric processes. Bull Am Meteorol Soc 56:527–530
Panofsky H, Dutton J (1984) Atmospheric turbulence models and methods for engineering applications. Wiley, New York
Petenko I, Argentini S, Casasanta G, Genthon C, Kallistratova M (2019) Stable surface-based turbulent layer during the polar winter at Dome C, Antarctica: sodar and in situ observations. Boundary-Layer Meteorol 171:101–128
Pfister L, Sayde C, Selker J, Mahrt L, Thomas CK (2019) Classifying the nocturnal boundary layer into temperature and flow regimes. Q J R Meteorol Soc 145:1515–1534
Rannik U, Vesala T (1999) Eddy covariance method; filtering; linear detrending; turbulent fluxes. Boundary-Layer Meteorol 91:259–280
Rees J, Denholm-Price J, King J, Anderson P (2000) A climatological study of internal gravity waves in the atmospheric boundary layer overlying the Brunt Ice shelf, Antarctica. J Atmos Sci 57:511–526
Rieder KF, Smith JA (1998) Removing wave effects from the wind stress vector. J Geophys Res 103:1363–1374
Salesky ST, Anderson W (2018) Buoyancy effects on large-scale motions in convective atmospheric boundary layers; implications for modulation of near-wall processes. J Fluid Mech 856:135–168
Salesky ST, Chamecki M, Bou-Zeid E (2017) On the nature of the transition between roll and cellular organization in the convective boundary layer. Boundary-Layer Meteorol 163:41–68
Schulz EW, Sanderson BG (2004) Stationarity of turbulence in light winds during the Maritime Continent Thunderstorm Experiment. Boundary-Layer Meteorol 111:561–577
Shah S, Bou-Zeid E (2014) Direct numerical simulations of turbulent Ekman layers with increasing static stability: modifications to the bulk structure and second-order statistics. J Fluid Mech 760:494–539
Shapiro A, Fedorovich E (2010) Analytical description of a nocturnal low-level jet. Q J R Meteorol Soc 136:1255–1262
Simiu E, Potra FA, Nandi T (2019) Determining longitudinal integral turbulence scales in the near-neutral atmospheric surface layer. Boundary-Layer Meteorol 170:349–355
Smeets C, Duynkerke P, Vugts H (1998) Turbulence characteristics of the stable boundary layer over a mid-latitude glacier, Part 1: a combination of katabatic and large scale forcing conditions. Boundary-Layer Meteorol 87:117–145
Smits AJ, McKeon B, Marusic I (2011) High-reynolds number wall turbulence. Annu Rev Fluid Mech 43:353–375
Sorbjan Z (1989) Structure of the atmospheric boundary layer. Prentice Hall, Englewood Cliffs
Sorbjan Z, Grachev A (2010) An evaluation of the flux-gradient relationship in the stable boundary layer. Boundary-Layer Meteorol 135:385–405
Sun J, Mahrt L, Banta RM, Pichugina YL (2012) Turbulence regimes and turbulence intermittency in the stable boundary layer during CASES-99. J Atmos Sci 69:338–351
Sun J, Mahrt L, Nappo C, Lenschow D (2015a) Wind and temperature oscillations generated by wave-turbulence interactions in the stably stratified boundary layer. J Atmos Sci 71:1484–1503
Sun J, Nappo CJ, Mahrt L, Belušić D, Grisogono B, Stauffer DR, Pulido M, Staquet C, Jiang Q, Pouquet A, Yagüe C, Galperin B, Smith RB, Finnigan JJ, Mayor SD, Svensson G, Grachev AA, Neff WD

(2015b) Review of wave-turbulence interactions in the stable atmospheric boundary layer. Rev Geophys 53(3):956–993. https://doi.org/10.1002/2015RG000487
Sun J, Lenschow DH, Mahrt L, LeMone MA, Mahrt L (2016) The role of large-coherent-eddy transport in the atmospheric surface layer based on CASES-99 observations. Boundary-Layer Meteorol 160:83–111
Tennekes H, Lumley JL (1972) A first course in turbulence. The MIT Press, Cambridge, p 300
Thomas CK, Kennedy A, Selker J, Moretti A, Schroth M, Smoot A, Tufillaro N (2012) High-resolution fibre-optic temperature sensing: a new tool to study the two-dimensional structure of atmospheric surface-layer flow. Boundary-Layer Meteorol 142:177–192
Van de Wiel BJH, Moene AF, Steeneveld GJ, Baas P, Bosveld FC, Holtslag AAM (2010) A conceptual view on inertial oscillations and nocturnal low-level jets. J Atmos Sci 67:2679–2689
Večenaj Ž, De Wekker SFJ (2015) Determination of non-stationarity in the surface layer during the T-REX experiment. Q J R Meteorol Soc 141:1560–1571
Vercauteren N, Mahrt L, Klein R (2016) Investigation of interactions between scales of motion in the stable boundary layer. Q J R Meteorol Soc 142:2424–2433
Vercauteren N, Boyko V, Kaiser A, Belušić D (2019) Statistical investigations of flow structures in different regimes of the stable boundary layer. Boundary-Layer Meteorol 173:143–164
Vickers D, Mahrt L (2007) Observations of the cross-wind velocity variance in the stable boundary layer. Env Fluid Mech 7:55–71
Yaglom A (1973) Stationary random functions. Dover, New York
Yagüe C, Cano J (1994) The influence of stratification on heat and momentum turbulent transfer in antarctica. Boundary-Layer Meteorol 69:123–136
Yagüe C, Viana S, Maqueda G, Redondo JM (2006) Influence of stability on the flux-profile relationships for wind speed, ϕ_m and temperature, ϕ_h, for the stable atmospheric boundary layer. Nonlinear Proc Geophys 13:185–203
Zeeman MJ, Selker JS, Thomas C (2015) Near-surface motion in the nocturnal, stable boundary layer observed with fibre-optic distributed temperature sensing. Boundary-Layer Meteorol 154:189–205